JOURNAL OF COMPUTATIONAL PHYSICS 77, 207–220 (1988)

Multi-cell Vortices Computed in Large-Scale Difference Solution to the Incompressible Euler Equations

ARTHUR RIZZI

FFA The Aeronautical Research Institute of Sweden,
S-161 11 Bromma, Sweden and
KTH, The Royal Institute of Technology,
S-100 44 Stockholm, Sweden

Received May 30, 1985; revised August 18, 1987

Large-scale computational results are presented for a three-dimensional flow containing a vortex sheet shed from a delta wing. A series of results computed under mesh refinement are compared with a vortex-element solution in which the vortex sheet is tracked as a non-diffusing discontinuity. The results are analyzed for the position of the vortex features captured in the Euler flowfield, the accuracy of the pressure field, and for the diffusion of the vortex sheet. The conclusions are that, with a sufficiently fine mesh, the dynamics of shed vortex flow are reasonably resolved and can be studied by grid-based solutions. The numerical solution indicates that the non-axisymmetric disturbance caused by the trailing edge of the wing sets up a torsional wave on the vortex core and produces a structure with multiple cells of vorticity. Although observed in coarse grid solutions too, this effect becomes better resolved with mesh refinement to 614,000 grid volumes. It is argued that this phenomenon is real, not numerical, and that it is not a form of vortex bursting. Instead, the conjecture is made that the phenomenon is the result of a vortex instability.

INTRODUCTION

Consider incompressible flow past a flat delta wing in which a stable[1] vortex sheet is shed from the leading edge and then coils up into a steady vortex over the wing (Fig. 1). We have investigated the qualitative as well as quantitative aspects of this flow, computed by artificial compressibility, in comparison to the results of a 3D panel method that fits the vortex sheet to the surrounding potential flowfield [1, 4]. The overall comparison between these two was quite favorable, but the Euler solution indicated a peculiar structure within the vortex core just ahead of the trailing edge that was not seen in the potential results. It raises the question of whether this feature is real in the sense that it belongs to the exact solution of the

[1] The stability analysis by Moore [11] shows that such a sheet is marginally stable to two-dimensional disturbances. In some cases experimental observation indicates that the sheet becomes unstable to three-dimensional disturbances.

0021-9991/88 $3.00

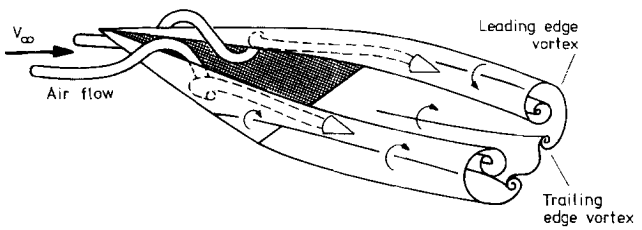

FIG. 1. Schematic of shed vortex sheets rolling up into stable vortex structures.

equations, or whether it is due only to the numerical method; i.e., the approximate solution is far from the exact one. There are, however, grounds to believe that such a curious feature on an otherwise conical vorticity field may in fact be physically realistic. It may well be the often-observed phenomenon of vortex bursting where the core of the vortex suddenly bellows out, and the circumferential velocity decreases dramatically. At the trailing edge the flow experiences a substantial upwash which lifts the vortex core and may cause it to burst.

The upwash gives curvature and therefore torsion [2] to the vortex core. This uplifting phenomena can be clearly seen in the vortex-element solution of Hoeijmakers [1] (Fig. 2), and it suggests a second possible mechanism at work to explain the curious structure in our numerical solution ahead of the trailing edge. The torsional force induced by the upwash may set in motion helical waves throughout the region of the vortex core. Under certain conditions such motion may become unstable and lead to the so-called multiple-vortex phenomenon [3]. It is conjectured here that the nonconical structure we found ahead of the trailing edge is real rather than numerical and that it is related to the multiple-vortex phenomenon. This paper attempts to test this hypothesis by the method of grid refinement in order to see if the sequence of solutions obtained on progressively finer and finer grids approaches some limit which can be considered close to the exact solution. The paper is a report on the findings of the refined-grid computations along with an interpretation of the results.

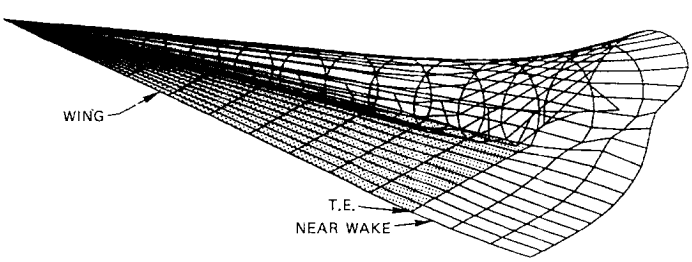

FIG. 2. The vortex sheet fitted as a discontinuity to the potential solution shows the curving of the vortex structure due to the upwash at the trailing edge.

Fine grids lead to computations on a very large scale that can consume all of the memory and several hours of time on current vector supercomputers. It is not uncommon to encounter computations involving several trillion arithmetic operations. In practice the size of the computer's real memory determines the degree of fineness of the computational mesh. Peripheral storage techniques, like an SSD unit, is a means around this, but it appears that its effectiveness is somewhat limited. All our calculations used only the real memory of the CYBER 205 with 16 M 32-bit words of storage. The grid was refined to fill the entire memory of the machine. Our previous solution was obtained on a medium-sized grid of $80 \times 24 \times 40$ cells [4]. The fine-mesh solution presented here using $160 \times 48 \times 80$ cells confirms, but in greater detail, the presence in the medium-mesh calculation of an azimuthal disturbance superposed upon the vortex core as it approaches the trailing edge of the wing. It is not altogether implausible that the shearing of the flow by the trailing edge causes this wave-like disturbance and the occurrence of the multi-celled vortex core.

Finite-Volume Method Using Artificial Compresssibility

The method used here has been presented before. The description now is only a brief outline. The equations of the artificial compressibility concept are solved using a spatially centered Runge–Kutta method in finite-volume form

$$\frac{\partial}{\partial t}\int q \,\mathrm{dvol} + M \cdot \iint \mathbf{H}\cdot\mathbf{n}\, ds = \Upsilon, \qquad M = \begin{vmatrix} c^2 & 0 & 0 & 0 \\ 0 & 1 & 0 & 0 \\ 0 & 0 & 1 & 0 \\ 0 & 0 & 0 & 1 \end{vmatrix}, \tag{1}$$

where $q = [p/\rho_0, u, v, w]$ and $\mathbf{H}\cdot\mathbf{n} = [\mathbf{V}\cdot\mathbf{n},\ u\mathbf{V}\cdot\mathbf{n} + p/\rho_0 \mathbf{n}\cdot\mathbf{e}_x,\ v\mathbf{V}\cdot\mathbf{n} + p/\rho_0\mathbf{n}\cdot\mathbf{e}_y,\ w\mathbf{V}\cdot\mathbf{n} + p/\rho_0\mathbf{n}\cdot\mathbf{e}_z]$ is the vector flux of q across the surrounding faces of the hexahedronal cells. The term Υ is a fourth-difference artificial-viscosity model. It has the property of an energy sink, i.e., $(d/dt)\, q^2 < 0$ summed over all the cells including those at the boundaries. The finite-volume method then discretizes (1) by assuming that q is a cell-averaged quantity located in the center of the cell, and the flux term $\mathbf{H}(q)\cdot\mathbf{n}$ is defined only at the cell faces by averaging the values on each side. With these definitions and calling the cell surfaces in the three coordinate directions of the mesh $\mathbf{S}_I$, $\mathbf{S}_J$, and $\mathbf{S}_K$, we obtain the semi-discrete finite-volume form for cell ijk,

$$\frac{d}{dt} q_{ijk} = -[\delta_I(\mathbf{H}\cdot\mathbf{S}_I) + \delta_J(\mathbf{H}\cdot\mathbf{S}_J) + \delta_K(\mathbf{H}\cdot\mathbf{S}_K)]_{ijk}$$

$$- \beta(\delta_I^4 + \delta_J^4 + \delta_K^4)\, q_{ijk} = \mathrm{FD}(q_{ijk}), \tag{2}$$

where $\delta_I(\mathbf{H}\cdot\mathbf{S}_I)\cong(\mathbf{H}\cdot\mathbf{S}_I)_{i+1/2}-(\mathbf{H}\cdot\mathbf{S}_I)_{i-1/2}$ is the centered difference operator and β is a constant in the range $0\leqslant\beta\leqslant 0.02$. The term FD is the discrete flux difference operator. Two types of boundary conditions are encountered in the problem: flow along the wing surface and the farfield boundary of the mesh. Because the wing is flat, the pressure gradient normal to the wing surfaces is zero. The leading edge itself introduces a geometric singularity from which the vortex sheet emanates. All flow gradients are large there, but their singular nature makes any estimate difficult. Therefore the method simple sets the pressure gradient to zero at the leading edge also. The velocity normal to the wing is set to zero, and the pressure is taken to be the same as that in all the mesh cells closest to the wing. In the farfield, the boundary conditions are determined by the appropriate combination of characteristic variables either extrapolated from the solution in the interior or given by the constant values of the freestream flow. This is a standard technique of absorbing boundary conditions that has been proven to work well. A more detailed description of the method is given in Refs. [4, 5].

With the appropriate boundary conditions we integrate Eq. (2) with the two-level three-stage scheme

$$
\begin{aligned}
q_0 &:= q \\
q &:= q_0 + \Delta t\ \mathrm{FD}(q_0) \\
q &:= q_0 + \Delta t[\tfrac{1}{2}\,\mathrm{FD}(q_0) + \tfrac{1}{2}\,\mathrm{FD}(q)] \\
q &:= q_0 + \Delta t[\tfrac{1}{2}\,\mathrm{FD}(q_0) + \tfrac{1}{2}\,\mathrm{FD}(q)]
\end{aligned}
$$

that steps the solution forward in time with a time step based on the stability limit local to each particular cell. Reference [4] derives the stability of the integration scheme from a Fourier analysis.

Tracked versus Captured Vortex Sheets

The greatest concern about the accuracy of a grid-based solution to the Euler equations for vortex dynamics is that the diffusion of vorticity may be too great. One way to maintain the diffusion at an acceptably low level is to grade the mesh in those regions where the vorticity is greatest. We attempt to do this with an O–O type mesh around the 70° swept flat-plate delta wing constructed by Eriksson's interpolation method [6] that places a polar singular line at the apex and a parabolic singular line at the tip of the trailing edge. The outer boundary is a hemisphere whose center is at mid rootchord of the wing and whose radius is 3 root-chord lengths. A subset of the mesh is drawn in Fig. 3 with 80 cells around the half span, 40 each on the upper and lower chord, and 24 outwards for a total of 76.800 cells. This particular grid topology focuses cells along the leading and trailing edges, as well as the apex where the flow changes most rapidly. It requires, however, a slight rounding of the wing tip. Hoeijmakers and Rizzi [1]

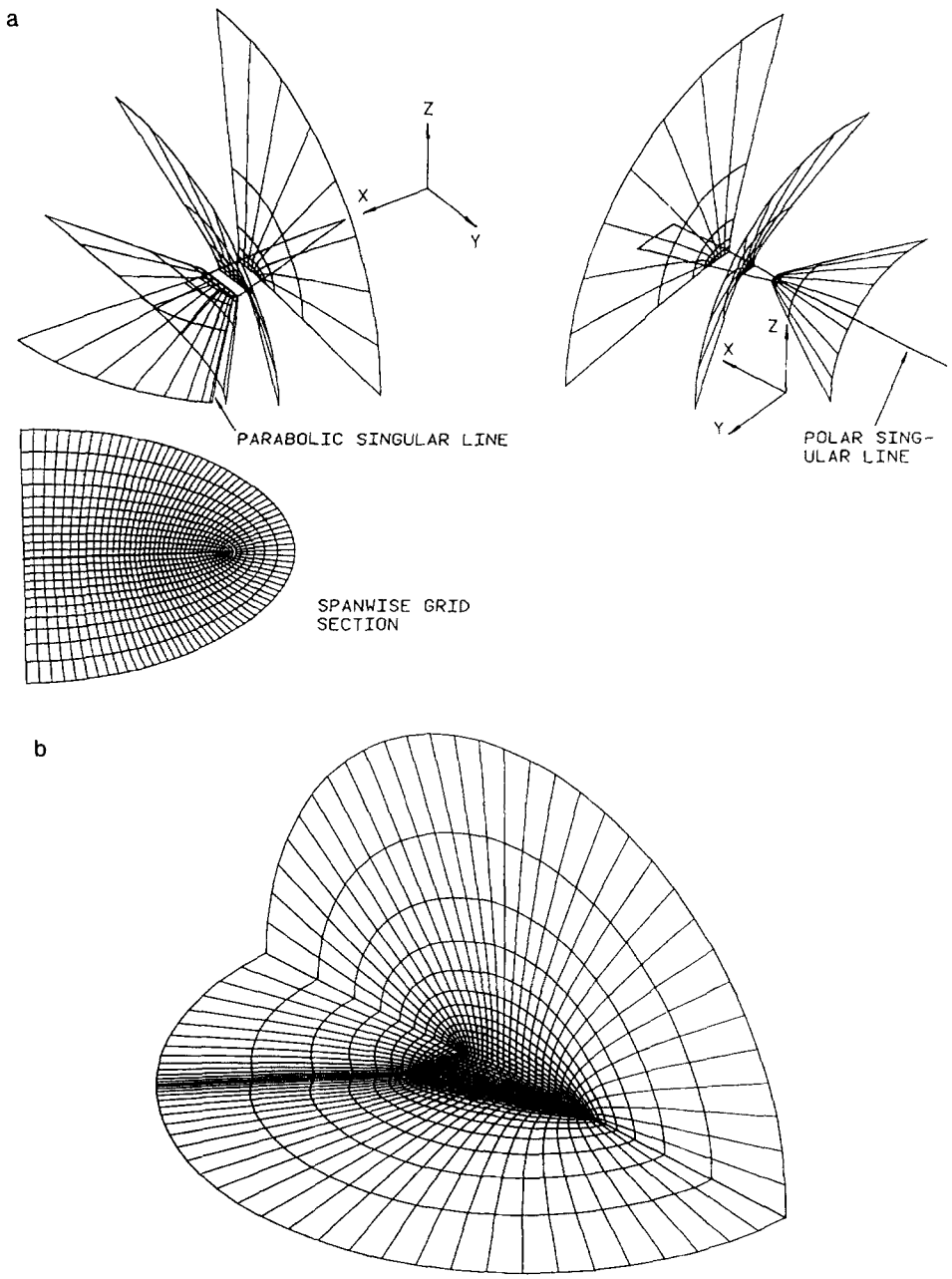

FIG. 3. (a) Grid generated around a delta-shaped small aspect ratio wing has an O–O topology. The polar singular line produces a dense and nearly conical distribution of points at the apex which is needed to resolve the rapidly varying flow there. This mesh is well-suited for computing the flow around wings of combat aircraft.

(b) Three-dimensional view of the delta wing mesh.

demonstrated that a stable vortex sheet can be captured in a numerical difference solution to Eq. (1) obtained upon this mesh which does agree well with a tracked non-diffusing vortex-element result (see also Ref. [4]). The captured Euler solution, however, indicates a wavelike structure superposed on the vortex core as it nears the trailing edge. A further question then arises, does the stability of the captured sheet, its close agreement in size and position with the non-diffusing one, and the observed wave structure all change as the mesh size is refined?

Hoeijmakers's potential boundary-integral (panel) method inserts a vortex sheet consisting of small panels or vortex elements, adjusts it to the surrounding irrotational flowfield, and allows it to roll up under its own influence for several turns, and then models the remaining core by an isolated line vortex [7]. The position and strength of the vortex sheet and isolated vortex are determined as part of the solution, sometimes termed "tracking or fitting" the rotational flow features. They are true discontinuities, infinitesimally thin, and for this reason a very good choice for comparison with a sheet and vortex smeared or "captured" over a number of computational cells. The comparison therefore offers a good check on the position of the computed vortex and the diffusion of the sheet as well as how these change with mesh size. Furthermore such panel-method results have been found to agree reasonably well with measurements made in turbulent flow [8].

Large-Scale Computation with Mesh Refinement

Where the flow, is smooth, the method is second-order accurate, but across discontinuities a formal estimate of accuracy loses meaning because the expansion upon which it is based breaks down. We might expect, however, the thickness of the rotational flow features captured in the solution to the Euler equations to vary in some manner with the size of the mesh cells. The simplest way, therefore, to minimize the diffusion of vorticity and to confirm the accuracy of the solution is to use as dense a mesh as possible. The large-scale computation presented here was carried out on a fine mesh with twice as many cells $160 \times 48 \times 80$ (over 600,000) as the previous solution [4], now called the medium-mesh results. The computations were carried out on the CYBER 205 vector computer in 32-bit precision at the rate of 6 μs per cell per iteration which translates to over 125 mflops. The results for the fine mesh have been integrated for 2500 time steps where the solution is steady. The working data set was nearly 14 M 32-bit words in size and resided entirely in real memory. Our experience indicates that it is very effective to run large-scale computations like these in a machine with ample real memory but under virtual-memory management. This is because at the start of the computations there are some intialization tasks that require additional scratch arrays, but which can be discarded after the iteration cycle has begun. At start-up practically 18 M words are needed, but the demand reduces to 14 M once the main cycle has begun. Virtual memory is one way to handle this initial overflow of 4 M words.

On the other hand, we have found it very ineffective to rely on virtual memory for the working set of the main iteration. This may well be due to the very slow disks of the CYBER 205, but it seems that even a faster unit like the SSD device has some limitations, as discussed by Bucher and Jordan [10]. They find that even though the hardware speed of the SSD is fast, large problems can still be I/O bound. This has to do with the balance between access and transfer times of the particular hardware unit, as well as with the size of the non-overlapped I/O operations and the buffer size. But it also seems to depend upon the software because in FORTRAN the buffers are filled by transfers of blocks of only 64 words at a time. Because of these uncertainties about its optimal performance I have not pursued the use of peripheral memory storage. Instead I have limited the mesh dimensions so that the working set resides entirely in main memory.

The overall features of the flows in the medium and the fine meshes are compared in Fig. 4 by isograms, drawn in plane projection, of the computed solution in three nonplanar mesh surfaces $x/c = 0.3$, 0.6, and 0.9 over the wing, one surface in the wake at $x/c = 1.15$ and one cutting axially through the core of the vortex. The two solutions do agree and reveal qualitatively the leading-edge vortex over the wing, as well as the trailing-edge vortex that develops from the trailing-edge sheet. The comparison shows that the broad features of the flow are represented in both grids and that they do not change substantially under mesh refinement. The isograms viewed along the axis of the core indicate the approximately conical nature of the flow starting at the apex. In both solutions at about 80% chord position, however, the leading-edge vortex lifts up slightly because of the rising pressure gradient beyond the trailing edge where the flow must eventually return to freestream pressure. This uplifting breaks the conical symmetry of the vortex and coincides with the asymmetric structure seen in the vorticity and total pressure fields ahead of the trailing edge (Figs. 4 and 5). Is this feature vortex bursting? Experiments with this wing have shown that bursting occurs over the wing at a higher angle of attack, about 30°. Also the characteristic trait of bursting is a sudden thickening or bellowing out of the vortex core. The results here do not seem to suggest vortex bursting.

Instead I favor another possible physical explanation. Since the pressure gradient beyond the trailing edge is increasing, it forces the vortex core to begin to lift up from the wing even before the edge. It gives the core curvature. Betchov's analysis then suggests that the core will spiral, and may become unstable. The most striking feature of these results is the abrupt change in the contour patterns that takes place ahead of the trailing edge between the two sections $x/c = 0.6$ and 0.9. It might be interpreted as a multi-celled vortex phenomenon. Although the cause of this feature may still be numerical, we should expect the core to undergo a helical disturbance physically that could excite an instability like the one discussed by Snow [3] which results in multiple vortices. At least it is a plausible explanation of the numerical results. In any event more of the local details are brought out in the fine mesh, but the streamwise position and overall dimension of the phenomenon does not change with mesh size.

No loss occurs in the total pressure in the tracked vortex-sheet solution, but sub-

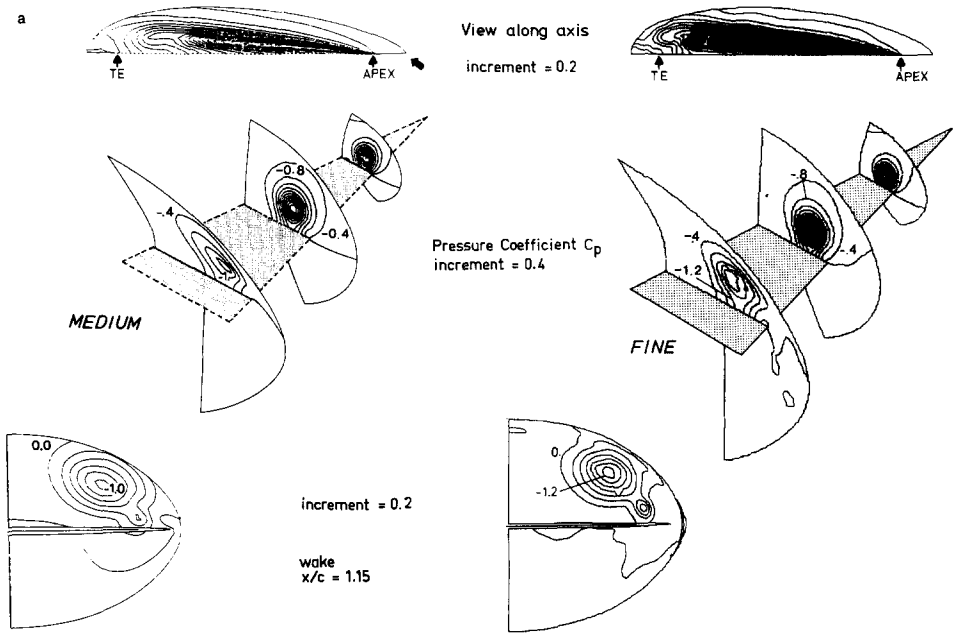
a
TE
APEX
View along axis
increment = 0.2
TE
APEX
-0.8
-.4
-0.4
MEDIUM
Pressure Coefficient C_p
increment = 0.4
-.8
-.4
-1.2
-.4
FINE
0.0
-1.0
increment = 0.2
wake
x/c = 1.15
0
-1.2

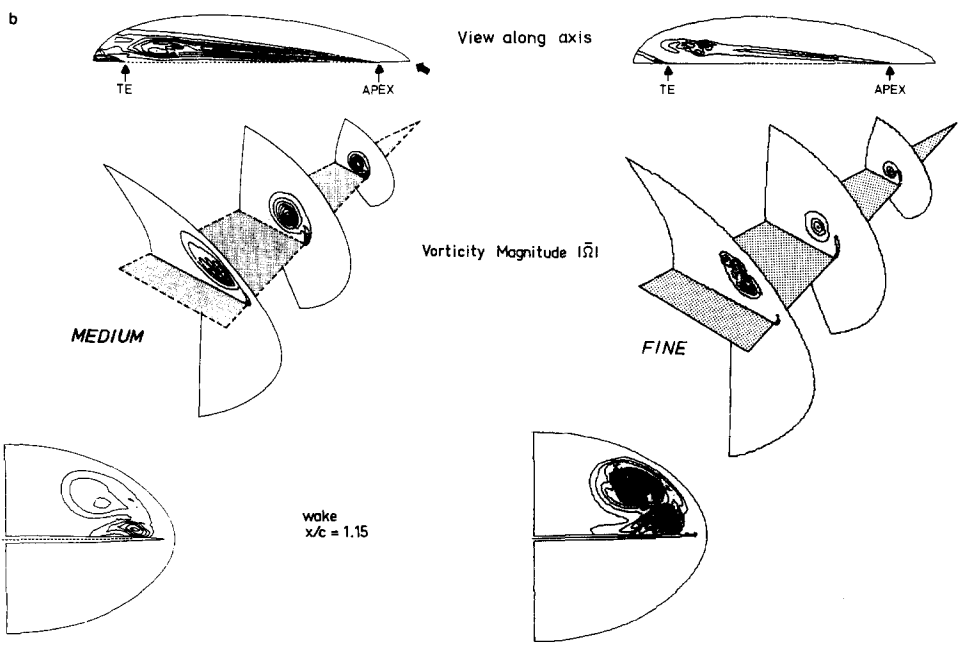
b
TE
APEX
View along axis
TE
APEX
MEDIUM
Vorticity Magnitude $|\bar{\Omega}|$
FINE
wake
x/c = 1.15

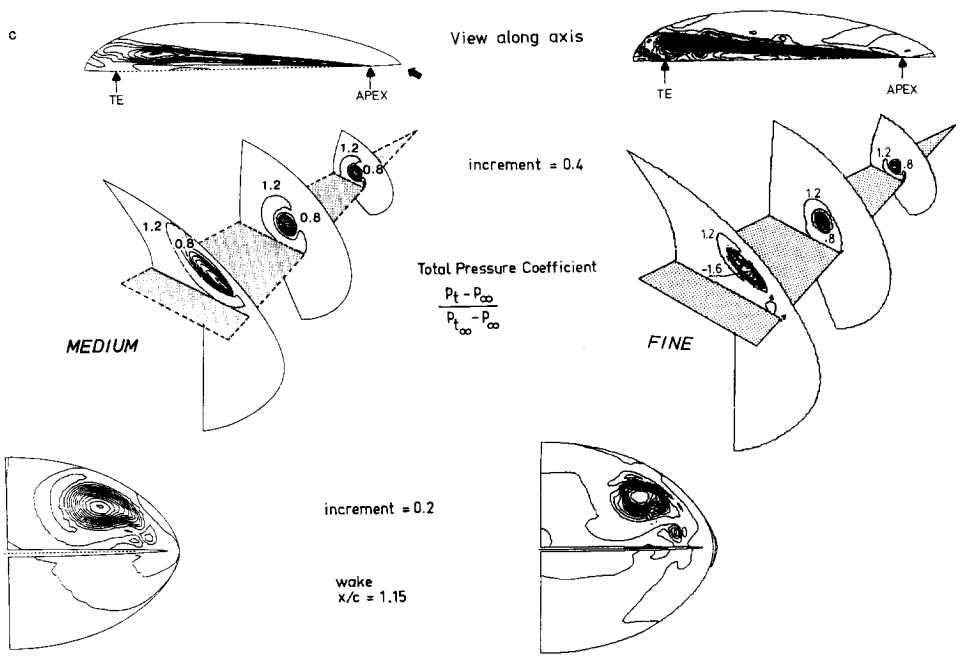

FIG. 4. Comparison of contour maps of the medium-mesh ($80 \times 24 \times 40$) and fine-mesh ($160 \times 48 \times 80$) solutions to the Euler equations (1) for flow past a 70° swept flat plate delta wing, They are drawn in four non-planar mesh surfaces at the $x/c = 0.3$, 0.6, 0.9, and 1.15 stations and in one mesh surface which passes approximately through the axial core of the vortex. $M_\infty = 0$, $\alpha = 20°$.

(a) Isobars of pressure coefficient C_p.

(b) Vorticity magnitude contours (not the same increment for medium and fine contours).

(c) Contours of total pressure coefficient. Increment = 0.4.

stantial losses do appear in my solutions where the sheet is captured over a number of mesh cells. The losses occur in two distinct locations and for different reasons. Near the leading edge of the wing the loss is attributed to the numerical effect of capturing the vortex sheet that is shed from the edge. Theoretically the loss should be zero on each side of the sheet, even though the velocity is in shear. But the numerical solution has to support this shear with a continuous profile over several mesh cells through the sheet, and any sort of reasonable profile (say a linear one) connecting the velocity vector on one side with the one on the other side immediately implies a total pressure loss for the profile even if the velocities at both sides are correct. This is the explanation given by Powell *et al.* [9]. The loss can be seen as an order-one error made in capturing the sheet. It is unavoidable and is just like the error that occurs when capturing a shock wave. What is important is to obtain the magnitude of the shear across the sheet reasonably correctly, just as one must calculate the jump in pressure across a shock correctly. And the comparison here with the tracked-sheet solution seems to suggest that this is the case.

The vortex core itself evolves from the sheet as it spirals inward tighter and

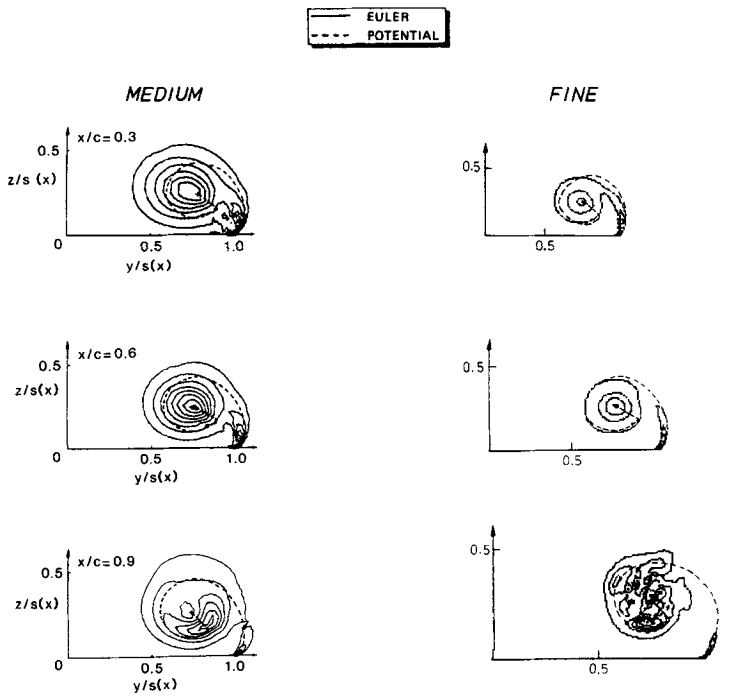

FIG. 5. Comparison of the vorticity fields indicated by vorticity magnitude contours (solid lines) computed with the Euler equations (1), using the medium and fine meshes, and the shed vortex (dashed lines) that is fitted as a discontinuity to the surrounding potential solution obtained by the 3D panel method.

tighter. This is a dissipative process, and since the method here is only artificially dissipative, the details cannot be correct. Moreover, with the kind of grid resolution offered here, even in the fine-mesh solution, barely one turn of the spiral is resolved before all trace of the jump in velocity shear is diffused into a region of smooth vorticity distribution. The vorticity reaches a maximum at the center of this region where the circumferental motion is transformed into axial motion. This region is the computed core, of which the local structure must be considered as fictitious. The essential role here of the artificial viscosity, or the truncation error, is to ensure that the circumferential or swirl velocity vanishes in the core. But the level of loss in total pressure found in the core is not random, it is set by the amount of shear produced at the leading edge which we believe is obtained with some accuracy through capture of the sheet. The amount of loss then is related directly to the strength of the sheet. The fine mesh supports more of the spiral, but the sheet must eventually disappear in this mesh too, in the same way, producing about the same loss at the center of a now smaller diameter core. It is the diameter therefore of the contour rings, but not their number, that varies with mesh spacing. In this way the

method always produces a viscous model of the core, which of course is not physically precise in its detail, but it does have the correct behaviour of reducing the swirl velocity to zero at the center of the core. We have seen and discussed this effect in the case of a compressible vortex flow also [12].

Figure 5 presents the shape of the tracked vortex sheet (dashed lines) from the potential method superimposed upon the vorticity magnitude contours of the Euler-equation solution in three cross-flow planes. We see when looking at the mesh in Fig. 3 that the vorticity captured in the field is diffused over 5 or 6 cells in both the medium and fine mesh solutions,[2] and that, in general, the vorticial flow region occupies a larger volume than that enclosed by the vortex sheet fitted to the potential solution. But the positions of the vortex cores in the comparisons and even the curvature of the sheets near the leading edge agree remarkably well. The vorticity in the fitted sheet is largest near the leading edge where the curvature of the sheet is singular, and the Euler-equation solutions indicate the same trend. The sheet appears to depart tangentially from the lower surface of the leading edge. This comparison with mesh refinement confirms that a stable vortex sheet separating from a swept leading edge can be captured in the vorticity field of the Euler-equation solution with a reasonable degree of realism. The curious distortion of the contours in the $x/c = 0.9$ station and the associated cellular pattern of vorticity are a better representation of the phenomenon in Fig. 4 which I called a standing torsional wave on the vortex core that gives rise to subsidiary vortices. Notice that the region of vorticity in this section does not bellow out appreciably, as one would expect if the vortex had actually burst. And the position and size of the vortical region does not change very much with mesh refinement. It is noteworthy to point out also that a previous computation of this flow with an even coarser mesh of $64 \times 20 \times 28$ cells revealed a similar feature at the same location and approximately the same size, but only with less detail [13]. This converging (but still not yet converged in the core) sequence of three computations strongly suggests that this feature ahead of the trailing edge belongs to the true solution of the equations.

Figures 6a, b present isograms on the wing surface together with the more quantitative graphs of spanwise distributions at three $x/c =$ constant stations and compare them with the potential values. In the sets of computed isobars (Fig. 6a) the pressure trough under the leading-edge vortex has about the same shape, position, and width, and the three agree rather well. The peak level of the suction along the entire trough on the upper surface is somewhat lower in the medium-mesh Euler results, and shifted slightly inboard at $x/c = 0.3$, but the fine-mesh results show a trend toward the potential solution. The fine-mesh results portray a pronounced waviness that may be a reflection of the character of the vortex as it approaches the trailing edge. A vortex core in helical motion might well produce such a pattern on the upper surface. This waviness, rather surprisingly, is not present in the circumferential $(v^2 + w^2)^{1/2}/V_\infty$ velocity components on the upper surface (Fig. 6b). The

[2] The increment between isovorticity contours is not the same for the medium- and fine-mesh solutions.

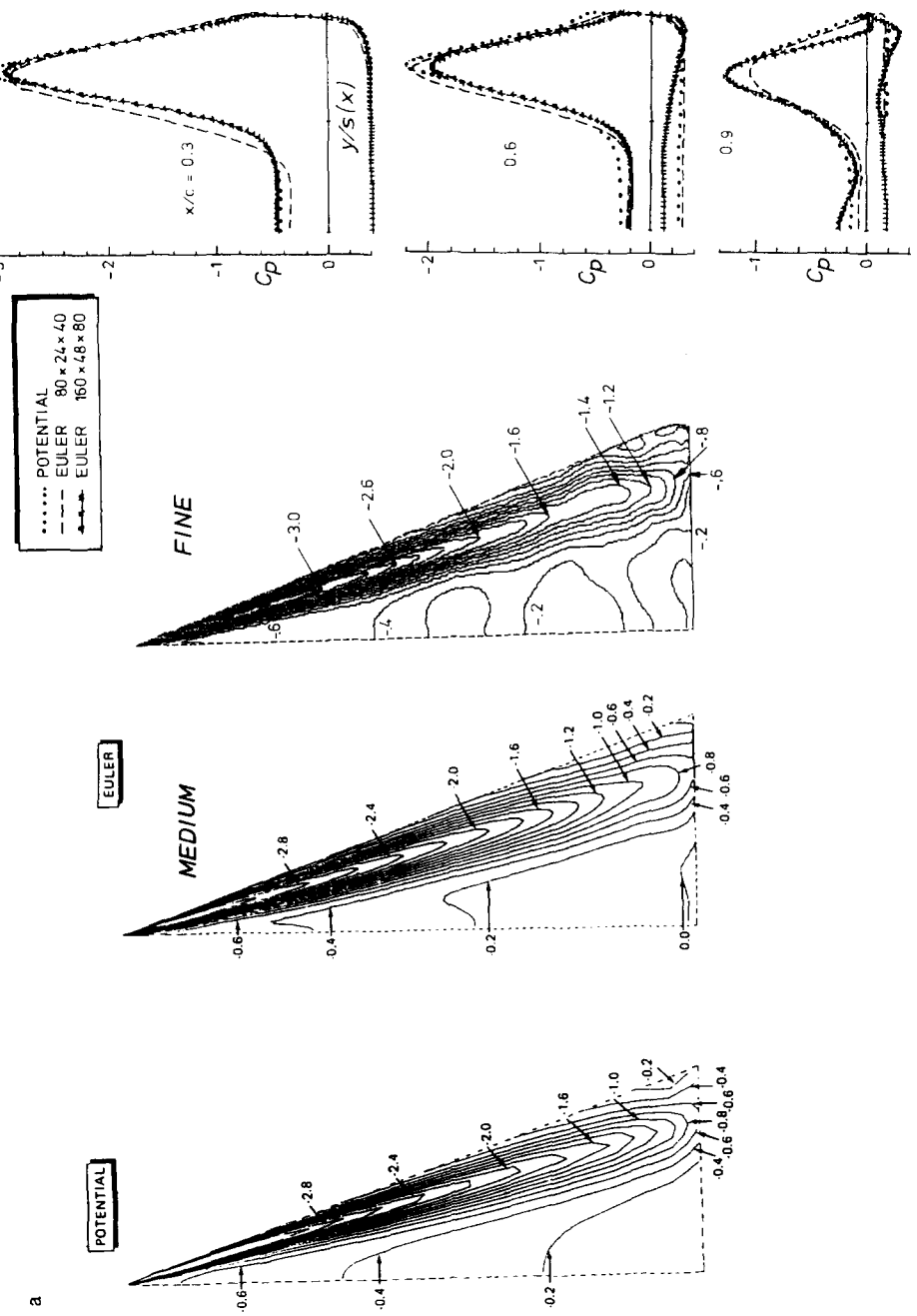
a
POTENTIAL
EULER
MEDIUM
FINE
..... POTENTIAL
— — — EULER 80 × 24 × 40
—•—•— EULER 160 × 48 × 80
x/c = 0.3
0.6
0.9
Cp
y/s(x)

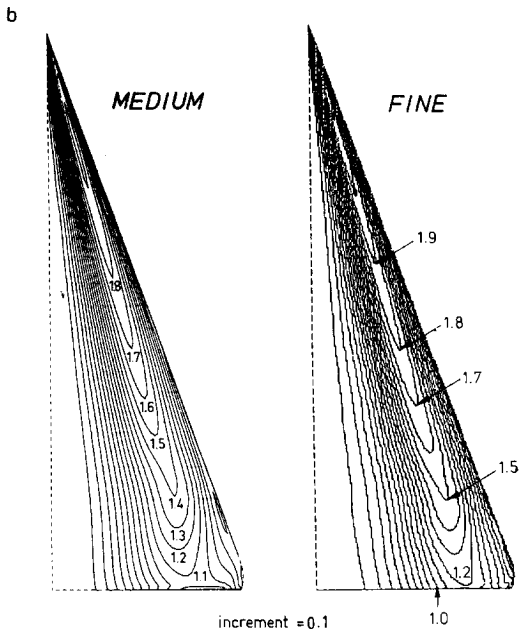

FIG. 6. Isograms of the computed medium-mesh and fine-mesh solutions to system (1) on the upper surface of the wing.

(a) Isobars of pressure coefficient C_p compared with the potential solution together with three corresponding graphs versus local semispan at $x/c = 0.3$, 0.6, and 0.9. Increment = 0.2.

(b) Circumferential velocity $(v^2 + w^2)^{1/2}/V_\infty$ contours.

contours of the circumferential velocity do reach a slightly higher value in the fine mesh than in the medium mesh, as one would expect, because the core is better resolved, the diffusion is less, and the swirl velocity is somewhat greater in the outer core region.

CONCLUDING REMARKS

The artificial compressibility approach is an interesting one for solving the incompressible Euler equations because it is equally applicable in small as well as large-scale simulations, and the latter provide a lot of insight into the local details of the flow. As a demonstration of the method, and as an example of a vortex flow requiring further understanding, a steady 3D flowfield with a free-shear layer has been computed, and its features have been discussed under grid refinement. Comparison with an accepted solution is reasonable, even though large (but local) errors in total pressure are observed, they do not seriously degrade the global accuracy of the solution and are shown to be an artifact of the numerical capturing

of the vortex sheet. A curious cellular pattern of vorticity in the core, coupled to a wave structure in the flow properties, also is seen to develop just ahead of the trailing edge of the wing and is believed to be caused by a three-dimensional disturbance on the vortex core. It is argued that this is not the phenomenon of vortex bursting because the vortical region does not suddenly bulge out. Instead the conjecture is that the three-dimensional disturbance of the trailing edge excites an instability that splits the core into several auxiliary vortices. At this time the reasoning remains speculative until it is either confirmed or refuted by further computations made using other meshes and carried out by other methods.

ACKNOWLEDGMENTS

I thank ETA Systems, Inc. for providing computer time for the further development of this method and Charles Purcell for his everpresent help in the running of the program. I am grateful to the second referee for his constructive and helpful comments.

REFERENCES

1. H. W. M. HOEIJMAKERS, AND A. RIZZI, Vortex-fitted potential solution compared with vortex-captured Euler solution for delta wing with leading edge vortex separation, *AIAA Pap.* **84-2144**, 1984.
2. R. BETCHOV, *J. Fluid Mech.* **22**, 471 (1965).
3. J. T. SNOW, *J. Atmos. Sci.* **35**, 1660 (1978).
4. A. RIZZI AND L. E. ERIKSSON, *J. Fluid Mech.* **153**, 275 (1985).
5. A. RIZZI AND L. E. ERIKSSON, *J. Fluid Mech.* **148**, 45 (1984).
6. L.-E. ERIKSSON, *AIAA J.* **20**, 1313 (1982).
7. H. W. M. HOEIJMAKERS AND W. VAATSTRA, *AIAA J.* **21**, 516 (1983).
8. H. W. M. HOEIJMAKERS, W. VAATSTRA, AND N. G. VERHAAGEN, *J. Aircraft* **21**, No. 9, 792 (1983).
9. K. POWELL, E. MURMAN, E. PEREZ, AND J. BARON, Total pressure loss in vortical solutions of the conical Euler equations, *AIAA Pap.* **85-1701**, 1985.
10. I. Y. BUCHER, AND T. L. JORDAN, *J. Comput. Phys.* **55**, 340 (1984).
11. D. W. MOORE AND R. GRIFFITH-JONES, *Mathematika* **21**, 128 (1974).
12. A. RIZZI AND C. J. PURCELL, *J. Fluid Mech.* **181**, 163 (1987).
13. A. RIZZI AND L.-E. ERIKSSON, in *Numerical Methods for the Euler Equations*, edited by F. Angrand *et al.* (Siam, Philadelphia, 1985), p. 437.